18th Brazilian Congress of Thermal Sciences and Engineering
November 16-20, 2020 (Online)l

# ENC-2020-0655
# ANALYSIS OF LIQUID-VAPOR INTERFACE VELOCITY USING OPTICAL FLOW METHOD DURING TWO-PHASE FLOW BOILING

**Jeferson Diehl de Oliveira**[1]
[1]University Center of Serra Gaúcha, Center of Innovation and Technology, Department of Mechanical Engineering, Os Dezoito do Forte, 2366, Caxias do Sul, 95020-472, RS, Brazil
jeferson.oliveira@fsg.edu.br; jeferson.physics@gmail.com

**Jacqueline Biancon Copetti**[2]
[2]University of Vale do Rio dos Sinos, Mechanical Engineering Graduate Program, LETEF, Laboratory of Thermal and Fluid Dynamic Studies, Unisinos Avenue, 950, São Leopoldo, 93022-750, RS, Brazil
jcopetti@unisinos.br; jacque.copetti@gmail.com

**Elaine Maria Cardoso**[3,4]
[3]UNESP – São Paulo State University, Post-Graduation Program in Mechanical Engineering, Av. Brasil, 56, 15385-000, Ilha Solteira, SP, Brazil
[4]UNESP – São Paulo State University, Campus of São João da Boa Vista, São João da Boa Vista, SP, Brazil
elaine.cardoso@unesp.br

***Abstract.*** *Flow patterns are found in many processes involving multiphase flows in the industry. This study experimentally investigated the behavior of the velocity field in the liquid-vapor interface during flow boiling of isobutane at a saturation temperature of 17 °C with heat flux varying from 5 to 20 kW/m² and fixed mass flux of 890 kg/(m²s). Tests were performed in a horizontal tube with an inner diameter of 1.0 mm. Four different flow patterns were identified based on images and the velocity fields in the liquid-vapor interface were investigated using an optical flow method.*

***Keywords:*** *two-phase flow, liquid-vapor interface, optical flow, velocity field, flow boiling*

## 1. INTRODUCTION

Several experimental studies have been performed to investigate characteristics of flow patterns due to their important influence on the performance of steam generators, evaporators and condensers. Thus, the study of the nonlinear dynamics of fluctuations of pressure drop is a significant contribution to understanding the flow patterns and instabilities observed in two-phase flow systems (Grzybowski and Mosdorf, 2014). In particular, many authors have focused their studies based on the dynamic of flow patterns, including superficial velocities and behavior of the liquid-vapor interface. Chen et al. (2012) investigated flow patterns of air-water in a condenser tube using a passive separation concept. The authors used an empty mesh cylinder inside the condenser, dividing the tube cross-section into an inner region and an annular region. Besides the results of superficial velocities, the morphologies of flow patterns were observed by image analysis and reconstructed in 3 dimensions. Kashid et al. (2012) developed an analytical model based on the flow stability analysis by Hickox (1971) in a concentric capillary tube with 1.6 mm ID using different fluids, including water, toluene, cyclohexane and different w% of glycerin. According to the authors, the two-phase flow was characterized in terms of the rate of perturbation with the axial velocity. And as result, the stability of annular flow was found to be increased with the increasing of Reynolds number and decreased in viscosity ratio of fluids introduced in the annular and core region.

A study of drop velocity based on image processing was implemented by Li et al. (2019). The characteristics of secondary droplets produced by a single drop impact on a liquid film were investigated using a high-speed camera with an acquisition rate of 5000 frames per second. The authors also used a pre-processing methodology of images to identify the dynamics of droplets and a particle tracking algorithm was implemented to calculate the velocity of such secondary droplets. As result, the authors observed variation of the number, diameter distribution and velocity distribution as functions of Weber number and the dimensionless film thickness. More recently, Eyal and Goldstein (2019) proposed the use of Green's function to solve the separated two-phase flow in inclined tubes. According to them,

such a method is based on an analogy to the electrostatic discipline that is composed of a superposition of the contributions created from an added driving force density, differently from the solution of Navier-Stokes.

Even considering that many studies have been reported in literature focusing on the behavior of flow patterns (Wang and Shoji, 2002; Klein et al., 2004; Revellin et al., 2006; Nguyen et al., 2010; Li et al., 2014; Tan et al., 2015; Rysak et al., 2016; O'Neill et al., 2018; Oliveira et al., 2020), there is a considerable lack of investigation on the nature of the behavior intrinsic to flow patterns during flow boiling in small channels. The main contribution of the present investigation is to analyze the liquid-vapor interface velocity with an optical flow method. The flow patterns were recorded using a high-speed camera. In turn, characteristics of interface velocity and vorticity are obtained.

## 2. EXPERIMENTAL FACILITY AND METHODOLOGY

An experimental setup was developed to investigate the flow boiling, pressure drop and flow patterns in a horizontal small channel. The details of such setup are shown schematically in Fig. 1. The experimental system consists of a loop that provides controlled mass flux, and it was designed to test different fluids under a wide range of flow conditions. The main part of the loop has a pre-heater PH, a test section TS and a visualization section VS. The secondary part consists of a condenser, a refrigerant reservoir, a liquid refrigerant vessel, a dryer filter, a magnetic gear pump and a subcooler. The condenser and the subcooler have independent circuits and each one uses an ethylene-glycol/water solution as the secondary refrigerant, the temperature of which is controlled by a thermostatic bath. This setup controls the refrigerant saturation temperature. The subcooler is used to compensate the temperature rise, which usually occurs as the refrigerant passes the gear pump, and also to assure that only subcooled liquid enters the flow meter. The PH establishes the experimental conditions entering the TS immediately downstream. It consists of a horizontal stainless-steel tube with a 1.0 mm internal diameter, a total length of 515 mm and a heated length of 440 mm. This tube is uniformly heated by direct application of an electrical current in the wall (Joule effect), the intensity of which is controlled by the power supplied by a SORENSENTM model DCS 8-125E, which provides both direct voltage and direct current measurements. The TS consists of the same tube and diameter with a total length of 366 mm, a heated length of 265 mm. As well as the PH, the TS is heated by the Joule effect, the intensity of which is controlled by the power supply.

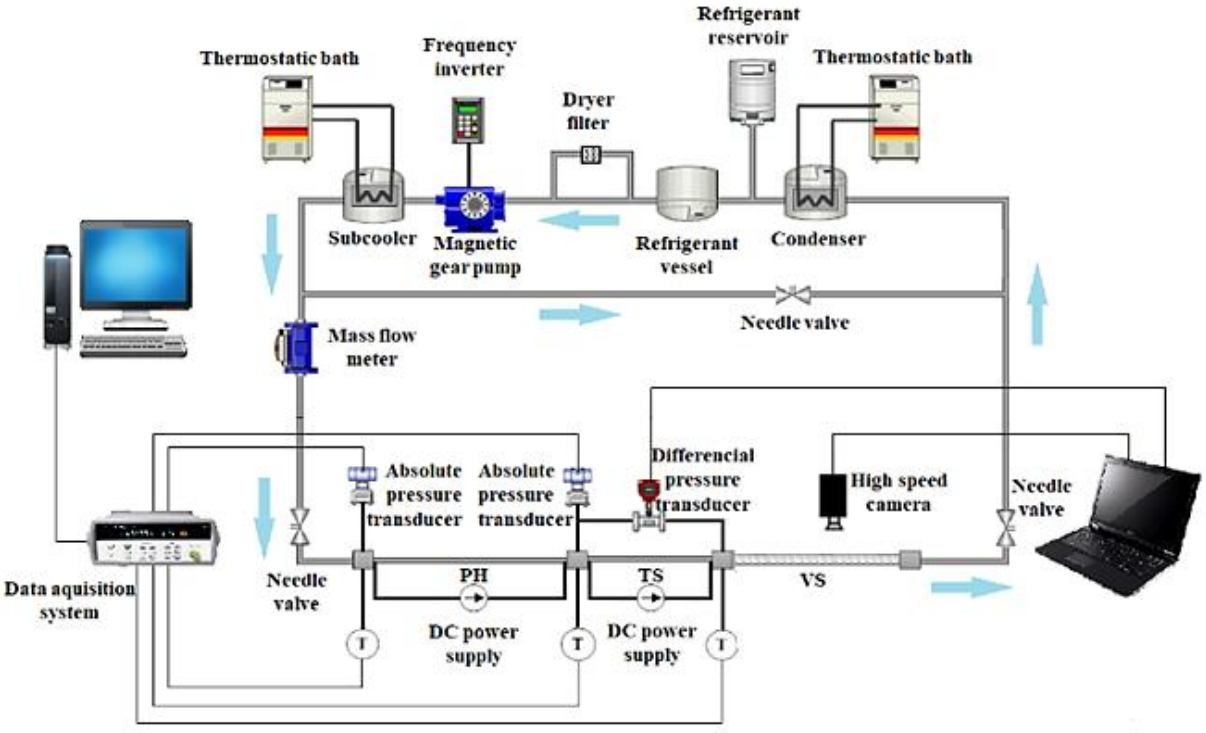


Figure 1 – Schematic of the experimental apparatus.

The absolute internal roughness ($R_a$) of the tube was measured with a STARRETTTM roughness tester, model SR 200, and was found to be 1.48 µm. There is a visualization section downstream of the TS with a 136 mm length glass tube with the same test section internal diameter. Both PH and TS are thermally insulated. The refrigerant enters the PH to establish a subcooled condition in the inlet of TS. In turn, this condition helps to reach different onset nucleate boiling (ONB) conditions based on mass and heat fluxes in the TS. Two 76 µm type-E thermocouples and two absolute pressure transducers, in contact with the refrigerant, measure temperature and pressure at both inlet and outlet of PH to

establish thermodynamic conditions. In TS both inlet and outlet temperatures are also measured. Absolute pressure transducers, mass flow meter, thermocouples and power meter were connected to an acquisition data system AgilentTM 34970A via RS 232 interface. All flow patterns were recorded with a high-speed camera MotionProTM Y4S1, using 9000 frames per second.

### 2.1 Data reduction

The heat flux applied to the test section was given by,

$$q''_{TS} = \frac{q_{TS}}{A_{heated}} \equiv \frac{U \cdot I}{\pi D_i L_{heated}} \tag{1}$$

where $D_i$ is the internal diameter, $L_{heated}$ is the heated length and, $U$ and $I$ represent the voltage and current applied by the power supply in the test section, respectively.

The vapor quality in the test section inlet was calculated from energy balance in the pre-heater, according to Eq. (2):

$$x_{(i-TS)} = \frac{\left(\frac{q_{PH}}{\dot{m}} + i_{i-PH}\right) - i_l}{i_{lv}} \tag{2}$$

where $i_l$ and $i_{lv}$ represent the liquid enthalpy and latent heat of vaporization as a function of saturation pressure.

Considering the local enthalpy as a function of location $z$ in the test section, given by:

$$i_{(z)} = \left(\frac{q_{TS(z)}}{\dot{m}} + i_{i-TS}\right) \tag{3}$$

Consequently, the local vapor quality along the test section was calculated according to:

$$x_{(z)} = \frac{i_{(z)} - i_l}{i_{lv}} \tag{4}$$

The void fraction was evaluated with the relation developed by Rouhani and Axelsson (1970). Thermodynamics and transport properties used in data reduction and pressure drop correlations were obtained from REFPROP v. 9.1 (Lemmon et al., 2013).

### 2.2 Optical Flow Method

The optical flow is based on the method developed by Liu and Shen (2008) considering the optical flow equation for different flow visualizations, which is given in terms of image coordinates:

$$\frac{\partial g}{\partial t} + \nabla \cdot (g\boldsymbol{u}) = f(x, y, g) \tag{5}$$

where $g$ represents the normalized image intensity that is proportional to the radiance received by the camera, $\boldsymbol{u} = (u_x, u_y)$ is the velocity in the image plane referred to as the optical flow and $f(x, y, g)$ corresponds to a boundary and diffusion term. The optical flow $\boldsymbol{u}$ is proportional to the light-path-averaged velocity weighted with the filed quantity $\psi$ related to a visualizing medium.

A variational formulation with a smoothness constraint is used to determine the optical flow, according to a functional given by Eq. (6):

$$j(\boldsymbol{u}) = \int_{\Omega} \left\{ \left[ \frac{\partial g}{\partial t} + \nabla \cdot (g\boldsymbol{u}) \right]^2 + \lambda \left( |\nabla u_x|^2 + |\nabla u_y|^2 \right) \right\} dxdy \tag{6}$$

where λ corresponds to the Lagrange multiplier and **Ω** is an image domain. By minimizing the Eq. (6), the Euler-Lagrange equation is obtained:

$$g\nabla\left[\frac{\partial g}{\partial t}+\nabla\cdot(g\boldsymbol{u})-f\right]+\lambda\nabla^2\boldsymbol{u}=0 \tag{7}$$

The solution of Eq. (7) is found using the standard difference method with Neumann condition $\partial\boldsymbol{u}/\partial n=0$ on the image domain.

## 3. RESULTS

Images collected with a high-speed camera were used to identify the flow patterns during the tests. To ensure the consistency of pattern analysis, two hundred images were obtained in each test, thus obtaining more than 2,000 images as a result of all tests. Four different flow patterns were observed: bubbly, plug, slug and churn. An example of bubbly flow is presented in Fig. 1. In fact, Fig. 1(a-b) shows a sequence of two pictures used to generate the global interface velocity field (Fig. 1(c)). The magnitude of the average velocity of the interface found in plug flow is 1.1 cm/s. It can be seen that negative vectors are presented at some points along with the flow. Such behavior can indicate the presence of vorticity in the liquid-vapor interface. Fig. 2 shows the normalized vorticity field along with the flow. Due to the buoyancy effect, bubbles are concentrated at the top of the channel and the effect of viscosity causes variations on velocity profile, causing vortexes mainly behind the bubble interfaces.

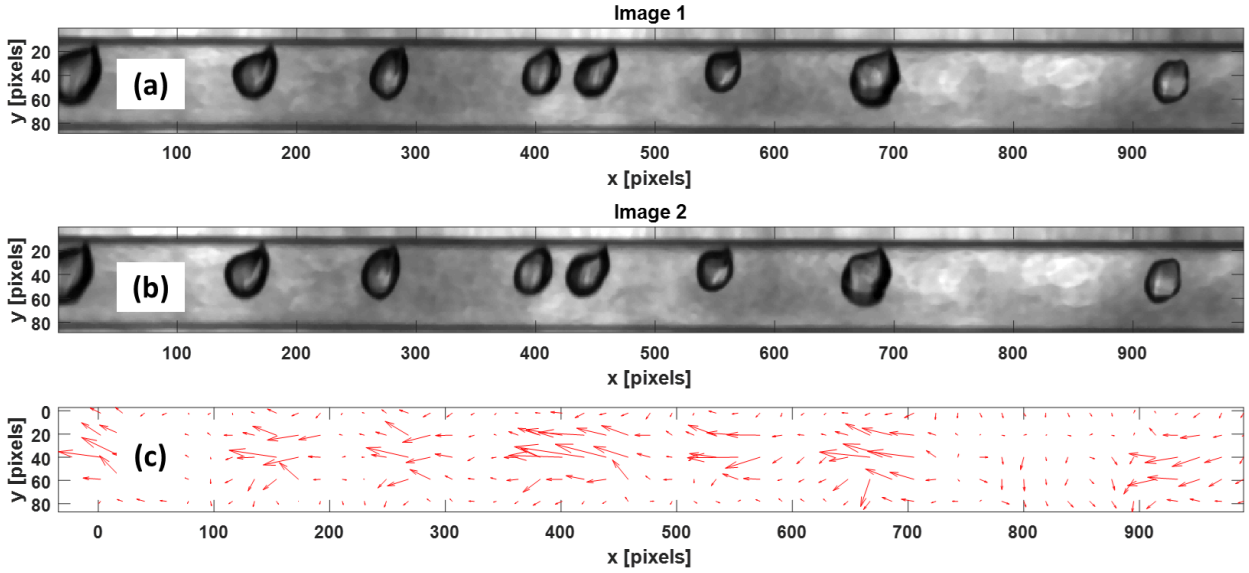


Figure 1 – (a-b) Bubbly flow obtained for the heat flux of 5 kW/m² and vapor quality of 0.01; (c) velocity field from optical flow.

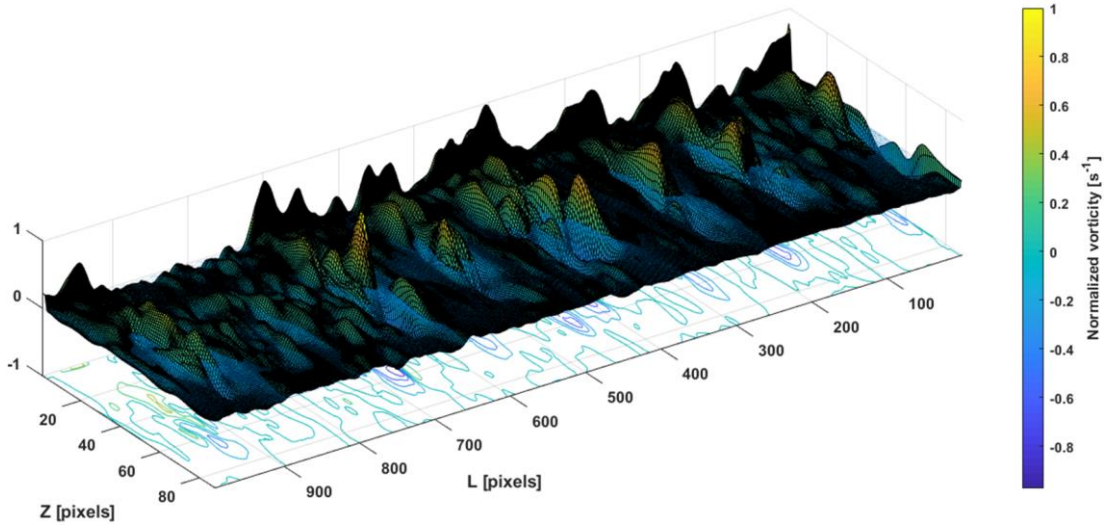


Figure 2 – Vorticity field of bubbly flow obtained for the heat flux of 5 kW/m².

An example of a plug flow pattern with the velocity field obtained from the optical flow method is presented in Fig. 3. In this case, plug flow is identified with small dispersed bubbles along with the flow. Fig. 3 (c) shows the global interface velocity field obtained from the analysis of both images. According to the results, the magnitude of the average velocity of the interface found in plug flow is 1.5 cm/s. On the other hand, dispersed bubbles have an average velocity of 0.6 cm/s, indicating that the vapor phase does not present a constant velocity. The analysis of the velocity field also indicates the presence of vorticity zones between plugs and among dispersed bubbles (Fig. 4). Such regions with vorticity can cause fluctuations of pressure along with the flow.

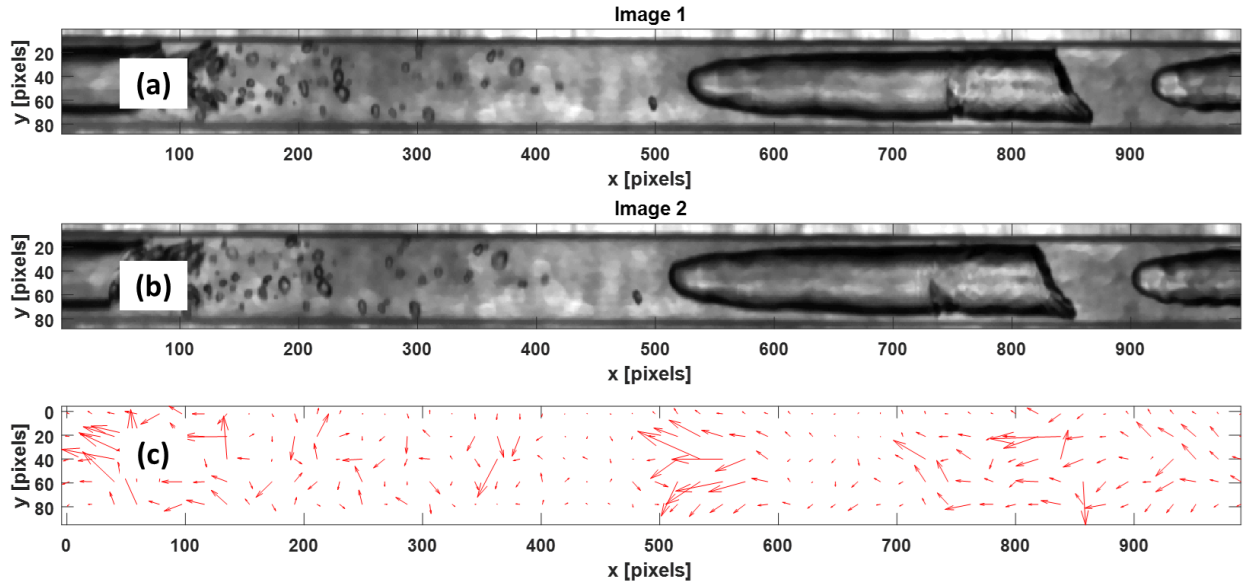


Figure 3 – (a-b) Plug flow obtained for the heat flux of 10 kW/m² and vapor quality of 0.1; (c) velocity field from optical flow.

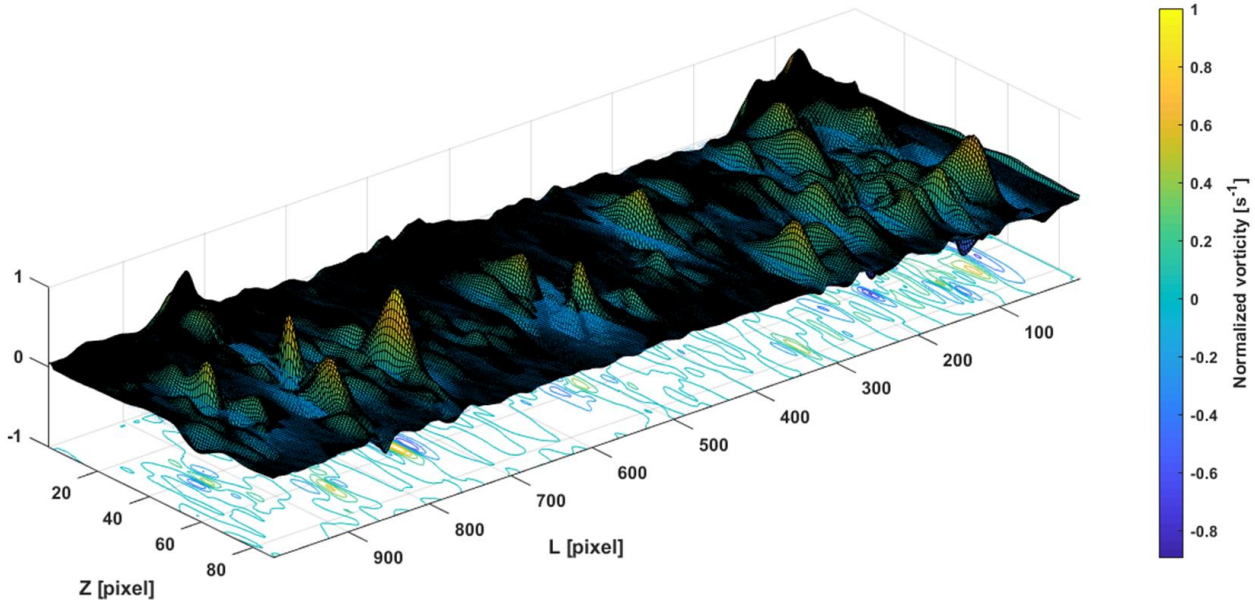


Figure 4 - Vorticity field of plug flow obtained for the heat flux of 10 kW/m².

The slug pattern is characterized as an “oblong nose” that protruded into the core and dispersion of bubbles from the tail, shown in Fig. 5 (a). Fluctuations of velocity field were also investigated along the *x*- and *y*-components in certain locations with fixed axial and radial directions. Fig. 5 (b) shows the behavior observed in the *x*-component of velocity at an axial position equal to 426-pixel (red line). In this case, such a velocity profile is observed in the tail of the slug where the bursting of bubbles creates regions with negative velocities. Churn flow regime was observed with a global interface in *y*-component of velocity ranging from -1,8 cm/s to 1,8 cm/s at a radial position equal to 44-pixel along with the flow (red line), according to Fig. 6 (b). The frequency of fluctuations of this component is caused by deformations in the interface (Kelvin-Helmholtz instability).

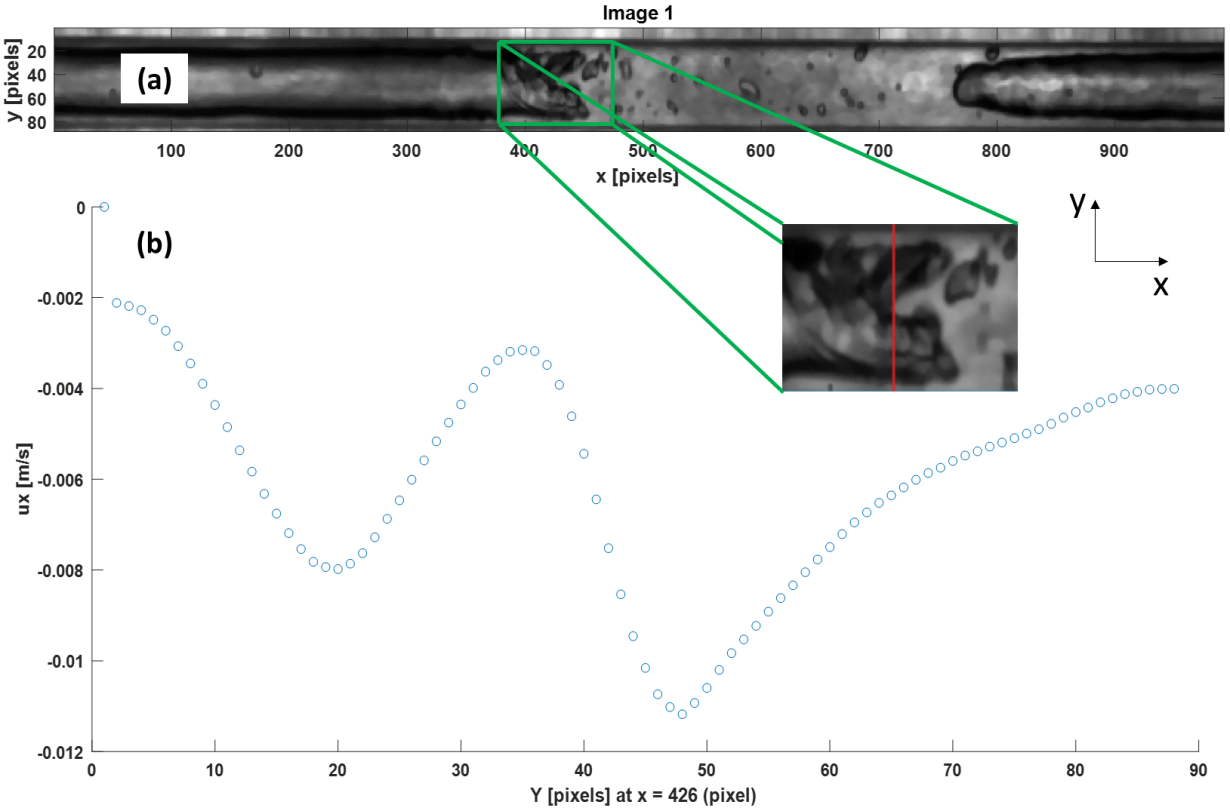


Figure 5 – (a) Slug flow obtained for the heat flux of 10 kW/m² and vapor quality of 0.24; (b) *x*-component of velocity along the radial direction.

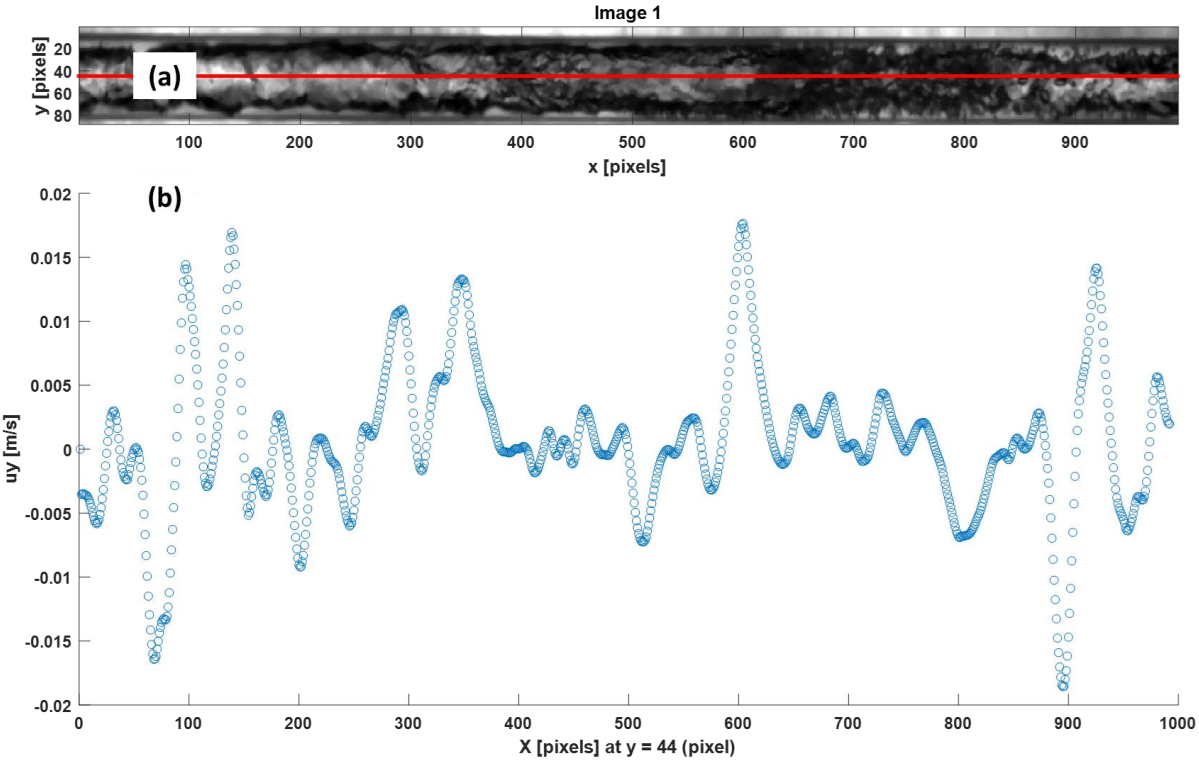


Figure 6 – (a) Churn flow obtained for the heat flux of 20 kW/m² and vapor quality of 0.53; (b) Component y of velocity along the axial direction.

## 4. CONCLUSION

The present investigation analyzed the liquid-vapor interface velocity of flow patterns from images provided by a high-speed camera during flow boiling of R-600a for a saturation temperature of 17 °C performed in a horizontal tube having an internal diameter of 1.0 mm. A method based on optical flow was used to determine the velocity fields. Besides the components of velocities, vorticity was identified along the flows caused by different velocities on the interface, causing deformations of patterns.

## 5. ACKNOWLEDGEMENTS

E. M. Cardoso acknowledges the contribution of PPGEM/FEIS - UNESP, CAPES, CNPq (458702/2014-5) and FAPESP (2013/15431-7 and 2019/02566-8).

## 6. REFERENCES

Chen, H., Xu, J., Li, Z., Xing, F., Xie, J., Wang, W., Wang, W. and Zhang, W., 2012. "Flow pattern modulation in a horizontal tube by the passive phase separation concept". *Int. J. Multiph. Flow*, Vol. 45, 12-23.

Eyal, O. and Goldstein, A., 2019. "Green's function method for solving the separated two-phase flow in inclined tubes with driving force contributions". *Int. J. Multiph. Flow*, Vol. 117, 103-113.

Grzybowski, H. and Mosdorf, R., 2014. "Dynamics of pressure oscillations in flow boiling and condensation in the minichannel". *Int. J. Heat Mass Trans*., Vol. 73, pp. 500-510.

Hickox, C.E., 1971. "Instability due to viscosity and density stratification in axisymmetric pipe flow". *Phys. Fluids*, Vol. 14, 251-262.

Kashid, M.N., Kowalinski, W., Renken, A., Baldyga, J. and Kiwi-Minsker, L., 2012. "Analytical method to predict two-phase flow pattern in horizontal micro-capillaries". *Chem. Eng. Sci*., Vol. 74, 219-232.

Klein, F.L., Seleghim Junior, P. and Hervieu, E., 2004. "Time-frequency analysis of intermittent two-phase flows in horizontal piping". *J. Brazilian Soc. Mech. Sci. Eng.*, Vol. 26, 174-179.

Lemmon, E.W., Hube, M.L. and McLinden, M.O., 2013. Physics and chemical properties division. REFPROP 9.1, NIST Standard Reference Database 23, Version 9.1

Li, H.W., Zhou, Y.L., Hou, Y.D., Sun, B. and Yang, Y., 2014. "Flow pattern map and time-frequency spectrum characteristics of nitrogen-water two-phase flow in small vertical upward noncircular channels". *Exp. Therm. Fluid Sci.*, Vol. 54, pp. 47-60.

Li, J., Zhang, H. and Liu, Q., 2019. "Characteristics of secondary droplets produced by a single drop impacting on a static liquid film". *Int. J. Multiph. Flow*, Vol. 2019, 42-55.

Liu, T. and Shen, L., 2008. "Fluid flow and optical flow". *J. Fluid Mech.*, Vol. 614, pp. 253-291.

Nguyen, V.T., Euh, D.J. and Song, C.-H., 2010. "An application of the wavelet analysis technique for the objective discrimination of two-phase flow patterns". *Int. J. Multiph. Flow*, Vol. 36, pp. 755-768.

Oliveira, J.D. Copetti, J.B., Passos, J.C. and var der Geld, C.W.M., 2020. "On flow boiling of R-1270 in a small horizontal tube: Flow patterns and heat transfer". *Appl. Therm. Eng.* Vol. 178, pp. 115403.

O'Neill, L. E., Mudawar, I., Hasan, M. M., Nahra, H. K., Balasubramaniam, R. and Mackey, J. R., 2018. "Experimental investigation of frequency and amplitude of density wave oscillations in vertical upflow boiling". *Int. J. Heat Mass Trans.*, Vol. 125, pp. 1240-1263.

Revellin, R., Dupont, V., Ursenbacher, T., Thome, J.R. and Zun, I., 2006. "Characterization of diabatic two-phase flows in microchannels: Flow parameter results for R-134a in a 0.5 mm channel". *Int. J. Multiph. Flow*, Vol. 32, pp. 755-774.

Rouhani, S.Z. and Axelsson, E., 1970. "Calculations of void volume fraction in the subcooled and quality boiling region". *Int. J. Heat Mass Transf.*, Vol. 13, pp. 383-393.

Rysak, A., Litak, G., Mosdorf, R. and Górski, G., 2016. "Investigation of two-phase flow patterns by analysis of Eulerian space-time correlations". *Int. J. Multiph. Flow*, Vol. 85, pp. 23-37.

Tan, C., Li, P., Dai, W. and Dong, F., 2015. "Characterization of oil-water two-phase pipe flow with a combined conductivity/capacitance sensor and wavelet analysis". *Chem. Eng. Sci.* Vol. 134, pp. 153-168.

Wang, S. and Shoji, M., 2002. "Fluctuation characteristics of two-phase flow splitting at a vertical impacting T-junction". *Int. J. Multiph. Flow*, Vol. 28, pp. 2007-2016.

## 7. RESPONSIBILITY NOTICE

The authors are the only responsible for the printed material included in this paper.